

The He star donor channel towards the black widow PSR J1953+1844

Yunlang Guo,^{1,2,3*} Bo Wang^{3,4,5†} and Xiangdong Li^{1,2‡}

¹*School of Astronomy and Space Science, Nanjing University, Nanjing 210023, China*

²*Key Laboratory of Modern Astronomy and Astrophysics, Nanjing University, Ministry of Education, Nanjing 210023, China*

³*University of Chinese Academy of Sciences, Beijing 100049, China*

⁴*Key Laboratory for the Structure and Evolution of Celestial Objects, Yunnan Observatories, Chinese Academy of Sciences, Kunming 650216, China*

⁵*International Centre of Supernovae, Yunnan Key Laboratory, Kunming 650216, China*

Accepted XXX. Received YYY; in original form ZZZ

ABSTRACT

Black widows (BWs) are a type of eclipsing millisecond pulsars (MSPs) with low companion masses ($\lesssim 0.05 M_{\odot}$) and tight orbits (< 1 d). PSR J1953 + 1844 (i.e. M71E) is a BW with the shortest orbital period (~ 53 minutes) ever discovered, which was recently detected by Five-hundred-meter Aperture Spherical radio Telescope. Its companion mass is $\sim 0.01 M_{\odot}$ according to its mass function, indicating that the companion may be a hydrogen-deficient star. However, the origin of PSR J1953 + 1844 is highly unclear. In this paper, we explored the origin of PSR J1953 + 1844 through the neutron star+He star channel, in which the system can experience ultracompact X-ray binary phase. We found that the He star donor channel can reproduce the characteristics of PSR J1953 + 1844, indicating that this work provides an alternative formation channel for this source. Meanwhile, the minimum orbital period of BWs formed by this channel is ~ 28 minutes, corresponding to the companion mass of $0.058 M_{\odot}$. In addition, we note that even though PSR J1953 + 1844 has a short orbital period, it cannot be detected by the gravitational wave (GW) observatories like Laser Interferometer Space Antenna, TaiJi and TianQin. However, we still expect that the BWs with extremely tight orbit produced by this channel are the potential sources of future space-based GW observatories. Moreover, our simulations show that PSR J1953 + 1844 may eventually evolve into an isolated MSP.

Key words: binaries: close – stars: individual: PSR J1953 + 1844 (M71E) – pulsars: general.

1 INTRODUCTION

Black widows (BWs) are a class of eclipsing millisecond pulsars (MSPs) orbiting together with low-mass companions ($\lesssim 0.05 M_{\odot}$; Roberts 2013; Chen et al. 2013; Benvenuto et al. 2014). It is generally believed that their companions are ablated by the wind resulting from the γ -ray illumination and the energetic particles radiated by MSPs, called the evaporation process (e.g. Kluzniak et al. 1988; Ruderman et al. 1989). They are important objects for revealing the evolutionary history of close neutron star (NS) binary systems, such as the decay of the surface magnetic field of NSs, the magnetic braking, the NS equation of state and the accretion efficiency, etc (e.g. Cumming et al. 2001; Tauris et al. 2012; Van et al. 2019; Godzieba et al. 2021; Li et al. 2021). In addition, it has been suggested that BWs may be a potential progenitor of isolated MSPs (e.g. van den Heuvel & van Paradijs 1988; Ginzburg & Quataert 2020; Guo et al. 2022). However, there is still no agreement on the origin of BWs (e.g. Chen et al. 2013; Benvenuto et al. 2014; Jia & Li 2015; Ablimit 2019; Guo et al. 2022).

Since the discovery of the first BW (PSR B1957+20; Fruchter et al. 1988), a large number of BW samples have been detected in the past decades. Recently, a BW pulsar, PSR J1953 + 1844 (i.e. M71E)

was discovered by the Five-hundred-meter Aperture Spherical radio Telescope (FAST) during the FAST Galactic Plane Pulsar Snapshot survey (Han et al. 2021), which has a spin period of 4 ms. Pan et al. (2023) obtained the orbital period of 53 minutes from the archival data of FAST globular cluster pulsar survey. The further timing shows that the mass of its companion is $\sim 0.01 M_{\odot}$ derived from the mass function of $2.3 \times 10^{-7} M_{\odot}$ (Pan et al. 2023). If the inclination angle ranges from 25.8° to 90° , the companion may be a hydrogen-deficient star, probably originating from ultracompact X-ray binaries (UCXBs; Yang et al. 2023). Pan et al. (2023) proposed a low mass X-ray binary channel with an evolved main sequence (MS) donor to explain the formation of PSR J1953 + 1844, that is, the mass-transfer process starts at the end of the MS phase of the donor. However, their model does not include the evaporation process that plays an important role in the formation of BWs and may widen the orbit.

The increasing number of detected BW samples indicate that they have two subtypes according to their companion mass (M_2): one is the BWs with $M_2 \sim 0.01 - 0.05 M_{\odot}$, and another is the BWs with $M_2 \lesssim 0.01 M_{\odot}$ (see Guo et al. 2022). Previous studies hardly explain the origin of the latter within the Hubble time (e.g. Chen et al. 2013; Ginzburg & Quataert 2020). Recently, Guo et al. (2022) further considered the evaporation process based on the He star donor channel forming UCXBs (see Wang et al. 2021). They reproduced the characteristics of the BWs with low-mass companions ($M_2 \lesssim 0.01 M_{\odot}$)

* E-mail:yunlang@nju.edu.cn

† E-mail:wangbo@yao.ac.cn

‡ E-mail:lixd@nju.edu.cn

and short orbital periods, such as PSRs J1719 – 1438, J2322 – 2650 and J1653 – 0158, etc.

Accordingly, the purpose of this paper is to investigate the formation of PSR J1953 + 1844 through the He star donor channel, in which the binaries can undergo the UCXB phase. In Section 2, we introduce the numerical methods for the binary evolution simulations and the adopted assumptions. In Section 3, we show the results of binary evolution and compare with observations. Finally, the relevant discussions and a summary are given in Sections 4 and 5, respectively.

2 NUMERICAL METHODS AND ASSUMPTIONS

We used the stellar evolution code Modules for Experiments in Stellar Astrophysics (MESA, version 12778; see Paxton et al. 2011, 2013, 2015, 2018, 2019) to carry out detailed binary evolution computations. We set the NSs as point masses, and the initial mass of NS is $M_{\text{NS}}^i = 1.4 M_{\odot}$. Meanwhile, since PSR J1953 + 1844 may locate in globular cluster M71, we constructed zero-age main-sequence He stars with two initial metallicities ($Z = 0.002, 0.02$). The initial mass of He star (M_2^i) and the initial orbital period are set to be $0.32 M_{\odot}$ and $P_{\text{orb}}^i = 0.013$ d, respectively. In addition, we adopted the Type-2 opacity tables suitable for the extra carbon and oxygen because of helium burning (Iglesias & Rogers 1996). We did not consider the magnetic braking usually used for the Sun-like star with a radiative core and a convective envelope (e.g. Rappaport et al. 1983; Chen et al. 2013; Paxton et al. 2015; Guo et al. 2022).

During the evolution of the NS+He star systems, the He star companion fills its Roche lobe as the orbit gradually shrinks owing to the gravitational wave (GW) radiation. The orbital angular momentum loss due to the GW radiation can be calculated by (Landau & Lifshitz 1971):

$$\frac{dJ_{\text{GR}}}{dt} = -\frac{32G^{7/2}}{5c^5} \frac{M_{\text{NS}}^2 M_2^2 (M_{\text{NS}} + M_2)^{1/2}}{a^{7/2}}, \quad (1)$$

in which the G , c and a are the gravitational constant, the speed of light in vacuum and the orbital separation, respectively. In addition, we used the ‘Ritter’ scheme to compute the mass-transfer rate (Ritter 1988). We assumed that the fraction of transferred material accreted by NS is 0.5, and set the Eddington accretion rate to be $3 \times 10^{-8} M_{\odot} \text{yr}^{-1}$ (e.g. Tauris & van den Heuvel 2006; Chen et al. 2011; Wang et al. 2021; Guo et al. 2023).

Lasota et al. (2008) suggested that for the irradiated pure helium discs, the thermal-viscous instability of accretion discs could be triggered if the mass-transfer rate is lower than $\sim 5 \times 10^{-10} M_{\odot} \text{yr}^{-1}$. At this moment, we assumed that the He star companion starts to be evaporated by the pulsar radiation. We used a simple prescription proposed by Stevens et al. (1992) to calculate the mass-loss rate of donor caused by the evaporation process:

$$\dot{M}_{2,\text{evap}} = -\frac{f}{2v_{2,\text{esc}}^2} L_{\text{P}} \left(\frac{R_2}{a} \right)^2, \quad (2)$$

where f , $v_{2,\text{esc}}$ and R_2 are the evaporation efficiency, the escape velocity at the donor surface and the donor radius, respectively. In this work, we calculated the binary evolution with different evaporation efficiencies, i.e. $f = 0, 0.01, 0.1$. $L_{\text{P}} = 4\pi^2 I \dot{P}_{\text{spin}} / P_{\text{spin}}^3$ is the spin-down luminosity of pulsars, in which $I = 10^{45} \text{ g cm}^2$ is the pulsar moment of inertia, P_{spin} and \dot{P}_{spin} are the spin period of pulsars and its derivative, respectively. We set the initial value of P_{spin} and \dot{P}_{spin} to be 3 ms and $1.0 \times 10^{-20} \text{ s s}^{-1}$, and used a constant braking index

(i.e. $n = 3$) to calculate the evolution of L_{P} (e.g. Chen et al. 2013; Jia & Li 2015).

3 RESULTS

3.1 A typical example for binary evolution

Fig. 1 shows a representative example of the evolution of a NS+He star system that can experience UCXB phase, in which we set the evaporation efficiency to be a typical value of 0.01. In the early stage of binary evolution, the rapid shrinking of the orbital separation is dominated by the loss of angular momentum owing to the GW radiation. At $t \sim 0.75$ Myr, the He star companion begins to fill its Roche lobe and the orbital period drops to 0.2 h, indicating that this binary system starts to appear as an UCXB (see Fig. 1a). At $t \sim 1.05$ Myr, the binary evolves to the minimum orbital period (~ 0.14 h) and the companion star decreases its mass to $\sim 0.30 M_{\odot}$. After that, the helium burning in the center of He star starts to fade and the He star gradually reaches a mildly degenerate state, indicating that this donor has a negative mass-radius exponent (see Wang et al. 2021).

At $t \sim 37.40$ Myr, the mass-transfer rate decreases to $\sim 5 \times 10^{-10} M_{\odot} \text{yr}^{-1}$, thus triggering the thermal-viscous instability of accretion discs. At this moment, the donor mass and the orbital period is $\sim 0.058 M_{\odot}$ and ~ 28.26 minutes, respectively. Meanwhile, the NS has accreted $\sim 0.1 M_{\odot}$ of material and spins up to become a MSP, resulting in that the donor begins to be evaporated by the pulsar radiation. From Fig. 1, we can see that the evaporation process increases the mass-loss rate of the donor, which could widen the orbital separation faster (e.g. Chen et al. 2013; Guo et al. 2022). The mass-transfer rate starts to increase at $t \sim 1$ Gyr, resulting from more rapid expansion of the degenerate He donor caused by the effective mass loss. In addition, we note that the mass of the donor can decrease to $< 10^{-2} M_{\odot}$ or even $< 10^{-3} M_{\odot}$ within the Hubble time.

3.2 Comparison with observations

We performed a series of complete binary evolution computations to reproduce the characteristics of PSR J1953 + 1844. Fig. 2 represents the evolutionary tracks of NS+He star systems with different f -values in the orbital period versus donor mass diagram. Meanwhile, PSR J1953 + 1844 may be located in globular cluster M71 (Pan et al. 2023), corresponding to a metallicity of 0.002 (Harris 1996). Thus, we also calculated the binary evolution with an initial metallicity of 0.002 for the He star companions. We note that for a given evaporation efficiency, the binaries have shorter orbital periods in lower metallicity. This is because lower metallicity leads to a smaller donor radius and mass-transfer rate, resulting in that the orbit expand more slowly (see, e.g. Wang & Han 2010). In addition, it is worth noting that our channel not only produces the BWs with low-mass companions ($M_2 \lesssim 0.01 M_{\odot}$; Guo et al. 2022), but also explains the BWs with ultra-compact orbits. The minimum orbital period of BWs that this channel can produce is ~ 28 minutes.

From Fig. 2, we can see that our simulations can explain the short orbital period and the low companion mass of PSR J1953 + 1844, indicating that this BW may originate from the He star donor channel. Meanwhile, our simulations show that PSR J1953 + 1844 may be produced by a evaporation efficiency of $\lesssim 0.1$. In addition, it is worth noting that PSR J1953 + 1844 does not show the eclipsing events in the observations, and Pan et al. (2023) speculated that its orbit is not edge-on. Nevertheless, this channel can still produce

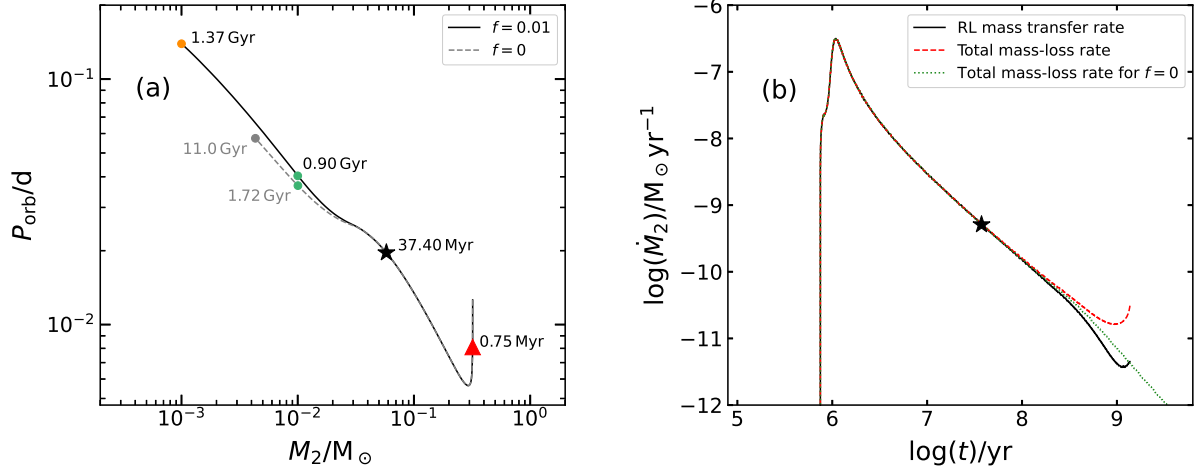


Figure 1. A typical example for the evolution of a NS+He star system that can undergo UCXB phase, in which $M_{\text{NS}}^i = 1.4 M_{\odot}$, $M_2^i = 0.32 M_{\odot}$, $P_{\text{orb}}^i = 0.013$ d, $Z = 0.02$ and $f = 0.01$. Panel (a): Evolutionary track of NS+He star system in the orbital period versus donor mass diagram. The red triangle and the black star indicate the moments when the mass transfer and the evaporation process start, respectively. The green and orange dots denote the moments when the donor mass decreases to $0.01 M_{\odot}$ and $0.001 M_{\odot}$, respectively. The gray dashed line denotes the evolutionary track of binary without evaporation process, and the code stops at $t \sim 11.0$ Gyr (the gray dot) because of hitting the equation-of-state limits (Wang et al. 2021). Panel (b): Evolution of mass-transfer rate (black line) and total mass-loss rate (red dashed line) as a function of time. The green dotted line denotes the evolutionary track of mass-loss rate for the model without evaporation process.

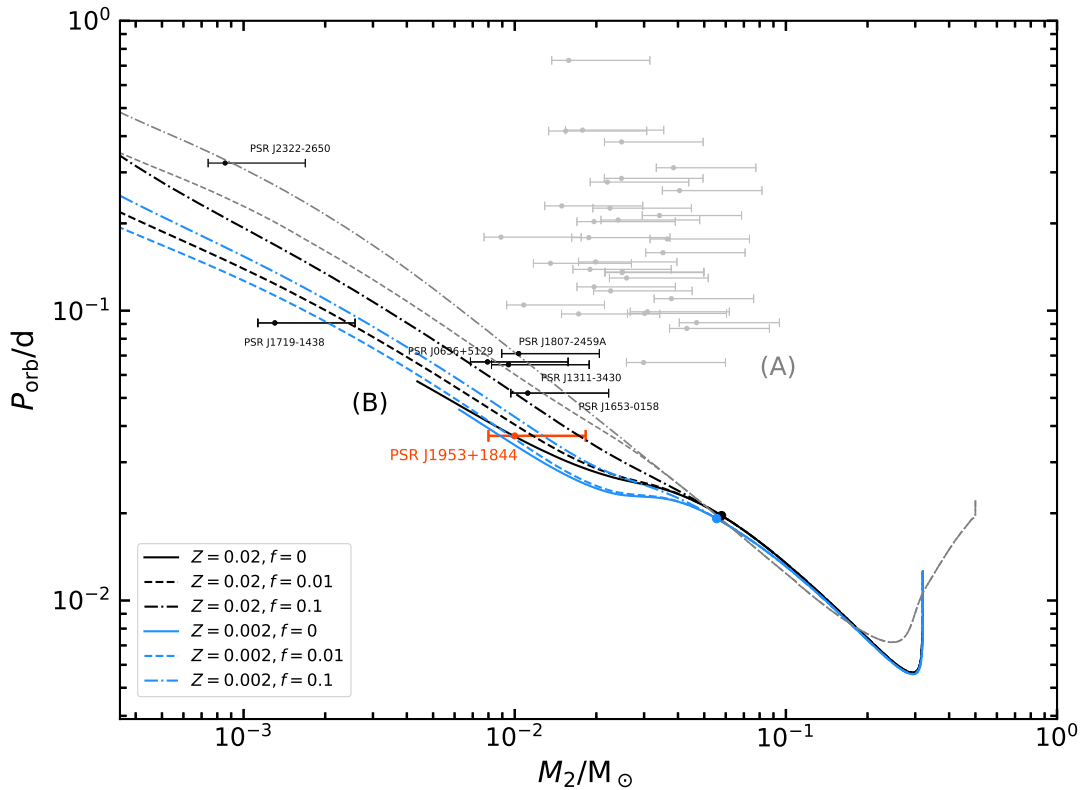


Figure 2. The evolutionary tracks of NS+He star systems with different f -values and metallicities (the black and blue lines) in the orbital period versus donor mass diagram, in which $M_{\text{NS}}^i = 1.4 M_{\odot}$, $M_2^i = 0.32 M_{\odot}$ and $P_{\text{orb}}^i = 0.013$ d. The blue and black dots indicate the moment when the evaporation process starts. The gray dashed and dashed-dotted lines represent the binary models with $(M_2, P_{\text{orb}}^i(d), f) = (0.5 M_{\odot}, 0.022, 0.01)$ and $(M_2, P_{\text{orb}}^i(d), f) = (0.5 M_{\odot}, 0.022, 0.1)$, in which the simulated data are taken from Guo et al. (2022). The red sample denotes PSR J1953 + 1844. The gray samples in region (A) are the BWs with $M_2 \sim 0.01 - 0.05 M_{\odot}$, and the black samples in region (B) are the BWs that can be explained by the He star donor channel. The left and right sides of the error bars correspond to the companion mass at orbital inclination angle of 90° and 26° (the 90% probability limit), respectively. The observed data are taken from the ATNF Pulsar Catalogue, <http://www.atnf.csiro.au/research/pulsar/psrcat> (version 1.70, 2023 May; Manchester et al. 2005).

the characteristics of PSR J1953 + 1844 even without evaporation. Therefore, the detected PSR J1953 + 1844 provides a strong support for the He star donor channel.

4 DISCUSSIONS

4.1 Gravitational wave signals

The detection of high-frequency GW signals from double black hole and double NS coalescence events open a new era of multimessenger astrophysics (GW150914 and GW170817; [Abbott et al. 2016, 2017](#)). On the other hand, the future space-based GW observatories (i.e. Laser Interferometer Space Antenna (LISA), TaiJi and TianQin) can be used to detect the low-frequency GW signals radiated by the inspiral processes of close binaries, such as UCXBs, AM CVn and double white dwarfs (WDs), etc (e.g. [Nelemans & Jonker 2010; Chen et al. 2020; Wang et al. 2021; Chen et al. 2022; Finch et al. 2023](#)). The recent detection of the BWs with short orbital periods (e.g. PSRs J1653 – 0158 and J1953 + 1844) indicate that the BWs may also be the potential sources of low-frequency GW. Thus, in this subsection, we discuss the possibility of BWs formed by this channel being detected by space-based GW observatories.

By considering that the GW signal is monochromatic, the characteristic strain amplitude of UCXBs based on 4 yr of LISA observations can be expressed as (e.g. [Tauris 2018; Chen 2020](#)):

$$h_c \approx 2.5 \times 10^{-20} \left(\frac{M_{\text{chirp}}}{M_{\odot}} \right)^{5/3} \left(\frac{f_{\text{GW}}}{\text{mHz}} \right)^{7/6} \left(\frac{15 \text{ kpc}}{d} \right), \quad (3)$$

in which $f_{\text{GW}} = 2/P_{\text{orb}}$ is the GW frequency, and d is the distance from the source to the detector. The chirp mass can be written as ([Tauris 2018](#)):

$$M_{\text{chirp}} = \frac{c^3}{G} \left(\frac{5\pi^{-8/3}}{96} f_{\text{GW}}^{-11/3} \dot{f}_{\text{GW}} \right)^{3/5}, \quad (4)$$

where \dot{f}_{GW} is the GW frequency derivative.

Fig. 3 shows the characteristic GW strain of the NS+He star binaries as a function of GW frequency, as well as the sensitive curves for LISA, TaiJi and TianQin (e.g. [Robson et al. 2019; Wang et al. 2019; Ruan et al. 2020](#)). We can see that metallicity and evaporation efficiency have no significant effect on the characteristic GW strains. In addition, the BWs originating from this channel cannot be detected by GW observatories if the distance exceeds 10 kpc. If we assume that PSR J1953 + 1844 is located in M71 (i.e. the distance is 4 kpc), then it cannot be visible as a low-frequency GW source (see the purple solid line). Table 1 shows the characteristics of binaries (i.e. the minimum donor mass and maximum orbital period) that can be detected by different detectors. Meanwhile, the parameter of the binaries at the beginning of evaporation is $(M_2, P_{\text{orb}}) = (0.058 M_{\odot}, 28.26 \text{ minutes})$. Accordingly, although the parameter space of the BWs that can be visible as GW sources is narrow, we still expect that the future space-based GW observatories will be helpful to detect the BWs with extremely short orbital periods.

4.2 Isolated MSP

At present, more than two hundred isolated MSPs have been detected. It is generally believed that BWs may be one of the progenitors of isolated MSPs, although the evolution process is still unclear (e.g. [van den Heuvel & van Paradijs 1988; Ginzburg & Quataert 2020; Guo et al. 2022](#)). Especially, two pulsars with planetary-mass companion ($M_2 \sim 10^{-3} M_{\odot}$) have been detected, i.e. PSR J1719 – 1438

Table 1. Characteristics of binaries that can be detected by different detectors. Dist is the distances from the source to the detectors; M_2^{min} and $P_{\text{orb}}^{\text{max}}$ are the minimum companion mass and the maximum orbital period of the binaries that can be detected by the detectors, respectively.

Detectors	Dist (kpc)	M_2^{min} (M_{\odot})	$P_{\text{orb}}^{\text{max}}$ (minutes)
LISA	1	0.026	38
	4	0.053	30
TaiJi	1	0.018	43
	4	0.040	34
TianQin	1	0.039	34
	4

([Bailes et al. 2011](#)) and PSR J2322 – 2650 ([Spiewak et al. 2018](#)), which may be two bridging objects between BWs and isolated MSPs. However, previous studies of evaporating the MS star with pulsar radiation is difficult to explain the formation of PSRs J1719 – 1438, J2322 – 2650 and the isolated MSPs within the Hubble time (e.g. [Chen et al. 2013; Ginzburg & Quataert 2020](#)).

[Ruderman & Shaham \(1985\)](#) suggested that He degenerate companion may experience the tidal disruption if its mass decreases to $\sim 10^{-3} M_{\odot}$.¹ Meanwhile, [Guo et al. \(2022\)](#) found that the companion mass can decrease to $< 10^{-3} M_{\odot}$ within the Hubble time for the He star donor channel, indicating that this channel is the potential progenitor of isolated MSPs. In this work, if we assume that the initial metallicity of the companion is 0.002 (i.e. PSR J1953 + 1844 is located in M71) and the evaporation efficiency is 0.01, then the companion mass will decrease from $0.01 M_{\odot}$ to $\sim 10^{-3} M_{\odot}$ after $\sim 0.50 \text{ Gyr}$. Accordingly, we expect that PSR J1953 + 1844 will eventually evolve into an isolated MSP.

4.3 Comparison to previous studies

It is still under highly debate for the companion nature of PSR J1953 + 1844. By assuming that the companion is a brown dwarf, [Pan et al. \(2023\)](#) concluded that the companion mass may range from $0.047 M_{\odot}$ to $0.097 M_{\odot}$ according to the mass-radius relationship. However, this mass range requires a narrow range of orbital inclination angle from 3.8° to 12.1° . On the other hand, the companion mass ranges from $8 \times 10^{-3} M_{\odot}$ to $15 \times 10^{-3} M_{\odot}$ based on its low mass function of $2.3 \times 10^{-7} M_{\odot}$, corresponding to a larger range of the orbital inclination angle from 25.8° to 90° (e.g. [Pan et al. 2023; Yang et al. 2023](#)). Thus, the companion of PSR J1953 + 1844 is more likely to have a low mass of $\sim 0.01 M_{\odot}$. In addition, the simulations of [Pan et al. \(2023\)](#) show that for the evolved MS donor channel, the binaries could undergo the UCXB phase, and the companion mass decreases to $\sim 0.01 M_{\odot}$ at $t \sim 10^{10} \text{ yr}$. Meanwhile, they claimed that PSR J1953+1844 may be the descendant of reback. [Conrad-Burton et al. \(2023\)](#) recently studied the evolved MS donor channel with a suitable magnetic braking model, and they found that orbital periods shorter than 1 h require significant fine-tuning.

In this work, the companions can decrease their masses to

¹ By approximately treating the donor as a zero-temperature and free degenerate gas, [Ruderman & Shaham \(1985\)](#) assumed that NS can tidally disrupt its He degenerate donor if $\frac{d \log R_L}{d \log M_2} > \frac{d \log R_L}{d \log M_2} \approx -\frac{1}{3}$, in which R_L is the Roche lobe radius of the donor related to the donor mass, NS mass, and orbital separation (see also [Stevens et al. 1992](#)).

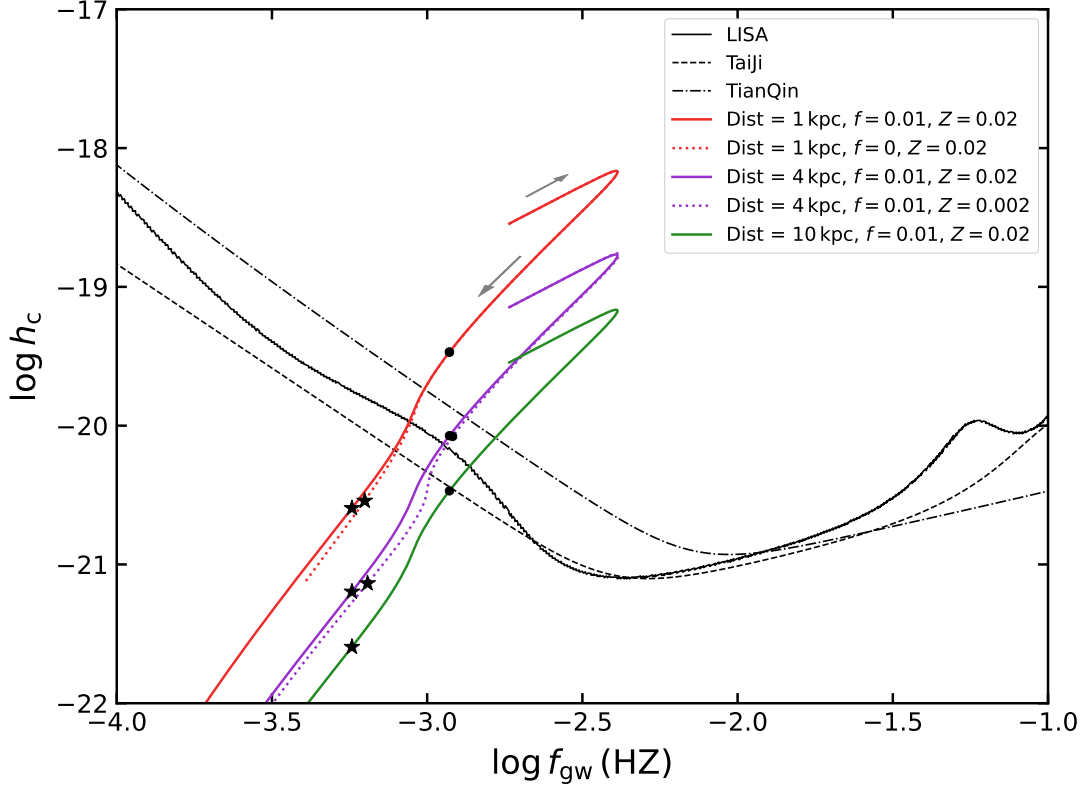


Figure 3. Evolutionary tracks of the NS+He star systems with different evaporation efficiencies, metallicities and the distances from the source to the detectors in the characteristic strain amplitude vs. GW frequency diagram, where $M_{\text{NS}}^i = 1.4 M_{\odot}$, $M_2^i = 0.32 M_{\odot}$ and $P_{\text{orb}}^i = 0.013$ d. The evolutionary tracks follow the direction of the gray arrows. The black dots and stars indicate the moments when the evaporation process starts and the companion mass decreases to $0.01 M_{\odot}$, respectively. The black solid, dashed and dashed–dotted lines represent the sensitive curves for LISA, Taiji and TianQin, respectively.

$\sim 0.01 M_{\odot}$ at $t \sim 10^9$ yr, and this time-scale is much shorter than that in Pan et al. (2023). Meanwhile, our simulations suggest that the progenitor of PSR J1953 + 1844 is an UCXB instead of a redback. In addition, the minimum orbital period of BWs in their simulations is ~ 38.68 minutes, which is slightly higher than our results (~ 28 minutes). Moreover, the minimum initial mass of the He star companions in this channel is $0.32 M_{\odot}$, which is the lower mass limit for He stars to ignite the central helium (Han et al. 2002). Thus, the surface of donors in our simulations shows the enrichment of the metal elements (e.g. C and O) after the evaporation process starts owing to the helium burning, and the abundance of metal elements increases with the initial mass of the He star donor. On the other hand, the donor ($M_2 \approx 0.01 M_{\odot}$) in Pan et al. (2023) has no metal enrichment, and is mainly composed of helium and hydrogen because the donor does not undergo the central helium burn (Chen H.-L. 2023, private communication). Furthermore, Yang et al. (2023) derived the evolutionary tracks of UCXBs to explain the properties of PSR J1953 + 1844 by using the analytical approach, and they suggested that its companion can be a CO WD or a He WD. More massive He star donor is needed if the companion of PSR J1953 + 1844 is a CO WD. It is expected that the future spectroscopic studies will provide more detailed properties for the companion of PSR J1953 + 1844.

5 SUMMARY

PSR J1953 + 1844 has the shortest orbital period (~ 53 minutes) among the detected BWs, and its companion mass is $\sim 0.01 M_{\odot}$ derived by its mass function. Using the stellar evolution code MESA,

we explored the origin of PSR J1953 + 1844 by considering the evaporation process based on the He star donor channel, where the binaries could experience the UCXB phase. Our simulations reproduce the characteristics of PSR J1953 + 1844, i.e. the low companion mass and the short orbital period. Thus, this work provides an alternative way for the origin of PSR J1953 + 1844, and implies that this object may originate from an UCXB. Meanwhile, we note that for the He star donor channel, the minimum orbital period of the formed BWs is ~ 28 minutes, corresponding to the companion mass of $0.058 M_{\odot}$. We then discussed whether the BWs formed by this channel can be detected by the future space-based GW observatories like LISA, Taiji and TianQin. We found that the GW observatories may be helpful for the detection of BWs with extremely short orbital periods. In addition, PSR J1953 + 1844 may evolve into an isolated MSP eventually, and this object provides a support for the He star donor channel.

ACKNOWLEDGEMENTS

We acknowledge the anonymous referee for the valuable comments that help to improve this paper. We thank Prof. Jinlin Han, Prof. Hailiang Chen, Zonglin Yang and Sivan Ginzburg for useful discussions and comments. This study is supported by the National Natural Science Foundation of China (Nos 12041301, 12121003 and 12225304), the National Key R&D Program of China (Nos 2021YFA0718500 and 2021YFA1600404), the Western Light Project of CAS (No. XBZG-ZDSYS-202117), the science research grant from the China Manned Space Project (No. CMS-CSST-2021-A12), the Yunnan

Fundamental Research Project (No. 202201BC070003), and the Frontier Scientific Research Program of Deep Space Exploration Laboratory (No. 2022-QYKYJH-ZYTS-016).

DATA AVAILABILITY

Results will be shared on reasonable request to corresponding author.

REFERENCES

- Abbott B. P., et al., 2016, *Phys. Rev. Lett.*, **116**, 061102
- Abbott B. P., et al., 2017, *Phys. Rev. Lett.*, **119**, 141101
- Ablimit I., 2019, *ApJ*, **881**, 72
- Bailes M., et al., 2011, *Science*, **333**, 1717
- Benvenuto O. G., De Vito M. A., Horvath J. E., 2014, *ApJ*, **786**, L7
- Chen W.-C., 2020, *ApJ*, **896**, 129
- Chen W.-C., Li X. D., Xu R. X., 2011, *A&A*, **530**, A104
- Chen H.-L., Chen X., Tauris T. M., Han Z., 2013, *ApJ*, **775**, 27
- Chen W.-C., Liu D.-D., Wang B., 2020, *ApJ*, **900**, L8
- Chen H.-L., Chen X., Han Z., 2022, *ApJ*, **935**, 9
- Conrad-Burton J., Shabi A., Ginzburg S., 2023, *MNRAS*, **525**, 2708
- Cumming A., Zweibel E., Bildsten L., 2001, *ApJ*, **557**, 958
- Finch E., et al., 2023, *MNRAS*, **522**, 5358
- Fruchter A. S., Stinebring D. R., Taylor J. H., 1988, *Nature*, **333**, 237
- Ginzburg S., Quataert E., 2020, *MNRAS*, **495**, 3656
- Godzieba D. A., Radice D., Bernuzzi S., 2021, *ApJ*, **908**, 122
- Guo Y.-L., Wang B., Han Z.-W., 2022, *MNRAS*, **515**, 2725
- Guo Y.-L., Wang B., Wu C.-Y., Chen W.-C., Jiang L., Han Z.-W., 2023, *MNRAS*, **526**, 932
- Han Z., Podsiadlowski P., Maxted P. F. L., Marsh T. R., Ivanova N., 2002, *MNRAS*, **336**, 449
- Han J. L., et al., 2021, *Research in Astronomy and Astrophysics*, **21**, 107
- Harris W. E., 1996, *AJ*, **112**, 1487
- Iglesias C. A., Rogers F. J., 1996, *ApJ*, **464**, 943
- Jia K., Li X.-D., 2015, *ApJ*, **814**, 74
- Kluźniak W., Ruderman M., Shaham J., Tavani M., 1988, *Nature*, **334**, 225
- Landau L. D., Lifshitz E. M., 1971, *Classical Theory of Fields* (Oxford: Pergamon Press)
- Lasota J. P., Dubus G., Kruk K., 2008, *A&A*, **486**, 523
- Li Z., Chen X., Chen H.-L., Han Z., 2021, *ApJ*, **922**, 158
- Manchester R. N., Hobbs G. B., Teoh A., Hobbs M., 2005, *AJ*, **129**, 1993
- Nelemans G., Jonker P. G., 2010, *New Astron. Rev.*, **54**, 87
- Pan Z., et al., 2023, *Nature*, **620**, 961
- Paxton B., Bildsten L., Dotter A., Herwig F., Lesaffre P., Timmes F., 2011, *ApJS*, **192**, 3
- Paxton B., et al., 2013, *ApJS*, **208**, 4
- Paxton B., et al., 2015, *ApJS*, **220**, 15
- Paxton B., et al., 2018, *ApJS*, **234**, 34
- Paxton B., et al., 2019, *ApJS*, **243**, 10
- Rappaport S., Verbunt F., Joss P. C., 1983, *ApJ*, **275**, 713
- Ritter H., 1988, *A&A*, **202**, 93
- Roberts M. S. E., 2013, in van Leeuwen J., ed., Vol. 291, *Neutron Stars and Pulsars: Challenges and Opportunities after 80 years*. pp 127–132 ([arXiv:1210.6903](https://arxiv.org/abs/1210.6903)), doi:10.1017/S174392131202337X
- Robson T., Cornish N. J., Liu C., 2019, *Classical and Quantum Gravity*, **36**, 105011
- Ruan W.-H., Liu C., Guo Z.-K., Wu Y.-L., Cai R.-G., 2020, *Nature Astronomy*, **4**, 108
- Ruderman M. A., Shaham J., 1985, *ApJ*, **289**, 244
- Ruderman M., Shaham J., Tavani M., 1989, *ApJ*, **336**, 507
- Spiewak R., et al., 2018, *MNRAS*, **475**, 469
- Stevens I. R., Rees M. J., Podsiadlowski P., 1992, *MNRAS*, **254**, 19P
- Tauris T. M., 2018, *Phys. Rev. Lett.*, **121**, 131105
- Tauris T. M., van den Heuvel E. P. J., 2006, in , Vol. 39, *Compact stellar X-ray sources*. pp 623–665, doi:10.48550/arXiv.astro-ph/0303456
- Tauris T. M., Langer N., Kramer M., 2012, *MNRAS*, **425**, 1601
- Van K. X., Ivanova N., Heinke C. O., 2019, *MNRAS*, **483**, 5595
- Wang B., Han Z., 2010, *A&A*, **515**, A88
- Wang H.-T., et al., 2019, *Phys. Rev. D*, **100**, 043003
- Wang B., Chen W.-C., Liu D.-D., Chen H.-L., Wu C.-Y., Tang W.-S., Guo Y.-L., Han Z.-W., 2021, *MNRAS*, **506**, 4654
- Yang Z. L., Han J. L., Jing W. C., Su W. Q., 2023, *ApJ*, **956**, L39
- van den Heuvel E. P. J., van Paradijs J., 1988, *Nature*, **334**, 227